

Threshold of coexistence and critical behavior of a predator-prey cellular automaton

Everaldo Arashiro and Tânia Tomé

Instituto de Física

Universidade de São Paulo

Caixa postal 66318

05315-970 São Paulo - SP, Brazil

(Dated: July 12, 2018)

We study a probabilistic cellular automaton to describe two population biology problems: the threshold of species coexistence in a predator-prey system and the spreading of an epidemic in a population. By carrying out time-dependent simulations we obtain the dynamic critical exponents and the phase boundaries (thresholds) related to the transition between an active state, where prey and predators present a stable coexistence, and a prey absorbing state. The estimates for the critical exponents show that the transition belongs to the directed percolation universality class. In the limit where the cellular automaton maps into a model for the spreading of an epidemic with immunization we observe a crossover from directed percolation class to the dynamic percolation class. Patterns of growing clusters related to species coexistence and spreading of epidemic are shown and discussed.

PACS numbers: 05.70.Ln, 87.23.Cc, 64.60.Ht

I. INTRODUCTION

In 1958, Huffaker [1], in a pioneering experiment, has been able to maintain in the laboratory a population of prey and predators coexisting and presenting self-sustained coupled time oscillations. He has verified that persistence of species was only possible in a large and heterogeneous space. Since then different models have been proposed to explain the rôle of space in determining the species coexistence [2, 3, 4, 5, 6, 7, 8, 9, 10, 11, 12, 13, 14]. A common feature of these models is that they are based either on interacting particle systems [15, 16], also called stochastic lattice models [4], or on probabilistic cellular automata. These descriptions are appropriate and relevant when considering predator-prey systems which are under conditions of very low species population densities and/or when their habitat is spatially heterogeneous [2].

In the present article we study a stochastic model that takes into account the spatial structure explicitly to describe two population biology issues: the threshold of species coexistence in a predator-prey system and the spreading of an infectious disease in a population. The individuals of each population are treated as discrete and they are supposed to occupy the sites of a two-dimensional lattice. The interactions between individuals are included in the local stochastic rules which take into account the Lotka-Volterra mechanisms of interaction [17, 18]. The dynamics associated to the system is a Markovian discrete time process defined by a probabilistic cellular automaton, having three states per site, which we call predator-prey cellular automaton. The connection between pattern formation and species coexistence in this model was recently analyzed [14]. Results from steady-state simulations have shown that, depending on the set of the parameters of the model, the following steady states can be attained [14]: a prey absorbing state, where predators have been extinct and the lattice is full of prey, and an active state where both species coexist with constant time densities. For finite systems, it

was also detected an active state where both population densities oscillate in time with the same characteristic frequency [11].

Our aim in this work is to determine with precision the threshold of stable coexistence of species in the predator-prey cellular automaton. To this end we perform time-dependent simulations [19, 20, 21, 22, 23, 24, 25, 26, 27, 28, 29, 30, 31] which allow us to obtain the phase boundaries together with the critical exponents. The scaling analysis of the time-dependent simulations yields a set of dynamic critical exponents and thus the possibility of classification of the models with absorbing states in universality classes. Here, we have found that the automaton exhibits a line of continuous phase transition which belongs to the universality class of directed percolation, for all sets of parameters such that the prey birth probability is different from zero. When this probability vanishes there occurs a crossover to the universality class of dynamic isotropic percolation. In this limit the predator-prey cellular automaton is mapped into a model for the spreading of an epidemic with immunization, a general epidemic process [20, 21, 32, 33, 34].

This article is organized as follows. In Sec. II we describe the predator-prey cellular automaton and the time-dependent simulations. Critical properties and pictures of growing clusters generated by the simulations are shown in the same section. In Sec. III we analyze the critical behavior of a model for an epidemic spreading. We briefly discuss and summarize our results in Sec. IV.

II. PREDATOR-PREY PROBABILISTIC CELLULAR AUTOMATON

A. The model

We assume that each individual of each species population can reside on the sites of a regular square lattice which represents their habitat. A site in the lattice can

be in one of three states: occupied by a prey individual (X); occupied by a predator individual (Y) or empty (Z). The predator-prey probabilistic cellular automaton comprehends the following processes:



and



The transitions between states obey probabilistic rules which depend on the state of the given site and on the states of its four nearest neighbors at the north, east, south and west (which defines the neighborhood). The update is synchronous and the rules are:

(i) A prey individual can be born in an empty site with a probability $a/4$ times the number of sites occupied by prey in the neighborhood, process (1).

(ii) A predator individual can be born in a site occupied by a prey if there are predators in its neighborhood. Prey disappear instantaneously and give place to a new predator. The probability of this process is $b/4$ times the number of sites occupied by predators in the neighborhood, process (2).

(iii) The death of predators is spontaneous: a site occupied by a predator can be evacuated with a probability c . This process reintegrates to the system the resources for prey proliferation, process (3).

The model has three parameters a , b , and c , with $0 \leq a \leq 1$, $0 \leq b \leq 1$ and $0 \leq c \leq 1$. However, we assume that $a + b + c = 1$, thus just two parameters are independent. We consider the parametrization [4, 14]: $a = (1 - c)/2 - p$ and $b = (1 - c)/2 + p$. The parameter p is such that $-1/2 \leq p \leq 1/2$ and parameter c denotes the death probability of predators, $0 \leq c \leq 1$. This parametrization allows us to analyze the model in a triangular phase diagram $p - c$, as shown in Fig. 1.

The system evolves in time and can eventually reach stationary states characterized by constant time densities of prey, predators, and empty sites. These can be either active states where prey and predators have stable coexistence or absorbing states. We note that finite systems also exhibit local oscillatory behavior of the densities of prey and predators [11].

A transition line $c_1(p)$ crosses the entire $p - c$ diagram represented in Fig. 1. It starts from the left corner of the triangle and ends on the opposite side. The densities of prey, predators and empty sites change continuously at $c_1(p)$. For $a \neq 0$, the transition is from the active state to the prey absorbing state and the transition line was estimated firstly in reference [14]. In the limiting case corresponding to $a = 0$, the point where $c_1(p)$ meets the right side of triangle of Fig. 1, the transition is from one of the infinitely many absorbing states to the prey absorbing state. In order to determine the critical line $c_1(p)$, with precision, and the dynamic critical exponents, we perform time-dependent simulations.

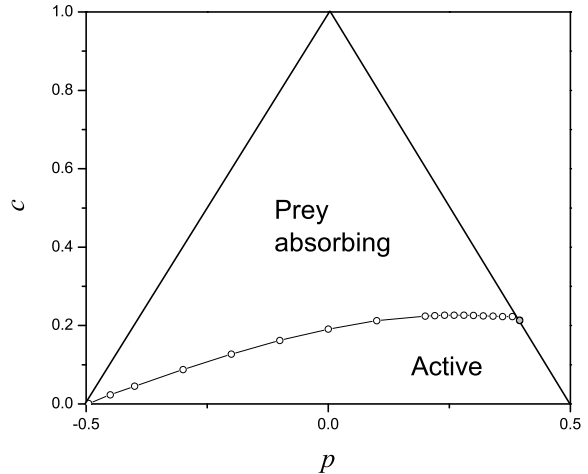


FIG. 1: Phase diagram in the plane $p - c$, showing regions corresponding to the prey absorbing phase and the active phase. Phases are separated by a transition line obtained from time-dependent simulations (see Table I).

B. Critical exponents and thresholds

To carry out a time-dependent simulation analysis for the predator-prey cellular automaton we follow the time evolution of states very close to the prey absorbing state. We depart from an initial condition ($t = 0$) with a single predator at the origin of a lattice covered by prey. Once the system is placed in the initial condition we apply the local rules (i), (ii), and (iii), described in Sec. II A, and let it evolve in time. We have considered $N_S = 10000$ samples (independent runs) all starting with this same condition. For each fixed value of p we vary c near its transition value. The simulations were performed in systems sufficiently large so that predators do not reach the borders of the lattice.

We have investigated the behavior of the following quantities: the survival probability of predators P , that is, the probability that predators have not been extinct until time t ; the mean-number of predators $\langle N \rangle$ at time t , whose average is calculated over all the samples, including those where predators have been extinct before time t ; and the average mean-square distance of spreading of predators from the origin, $\langle R^2 \rangle$. This average is calculated by taking into account only the samples that survived until time t .

According to the scaling laws for time-dependent simulations [19], for large values of t , we expect, at the critical point, the following power laws,

$$\langle N \rangle \sim t^\eta, \quad (4)$$

$$P \sim t^{-\delta}, \quad (5)$$

and

$$\langle R^2 \rangle \sim t^z, \quad (6)$$

where η , δ and z are the critical exponents associated to the mean-number of predators, the survival probability, and the mean-square distance of spreading, respectively.

As can be seen in Fig. 2, the log-log plot of the mean-number of predators, as well as of the survival probability, show very well defined critical and off-critical asymptotic behaviors. For a fixed value of p , and values of c below, but close to the critical value (supercritical regime), these quantities present a positive curvature, which indicates the presence of activity in the system; and for values of c greater than the critical value (subcritical regime) they present a negative curvature. At criticality, $\langle N \rangle$ and P exhibit a very clear asymptotic power law behavior. Therefore, it is possible to obtain, with precision, the phase boundaries together with the critical exponents. From Fig. 2 we get the following estimates for the critical exponents

$$\eta = 0.230(2), \quad \delta = 0.451(3), \quad z = 1.134(4),$$

for $p = 0$ (that is, for $a = b$). As reported in Table I, the same values for the exponents, with the error bars, were obtained (using the same procedure) for different values of p along the critical line $c_1(p)$ (excluding the critical point for which $a = 0$). The errors of the exponents were estimated by dividing $N_S = 10000$ samples in bins of 2000 runs, and calculating the fluctuation of the averages obtained for each bin. These values of the dynamic critical exponents are consistent with the ones of the directed percolation class in $2+1$ dimensions: $\eta = 0.2295(10)$, $\delta = 0.4505(10)$ and $z = 1.1325(10)$ [29].

This dynamic critical behavior has been obtained for a diversity of models with finite number of asymmetric absorbing states [27, 29], such as the contact process, which can be viewed as a model for a simple epidemic [15]. The critical behavior of this model has been extensively studied and it belongs to the directed percolation class [26, 27, 28]. Other examples are the Domany-Kinzel cellular automaton [35] and the spreading of damage transitions [27, 36, 37]. Among the models with more than one absorbing state, perhaps the most known is the Ziff-Gullari-Barshad model [38] for the reaction of oxidation of carbon monoxide over a catalytic surface; it also has dynamic critical exponents [24] consistent with the ones associated to the directed percolation class.

The critical exponent associated to the time correlation length ν_{\parallel} can be obtained from the time-dependent simulations. Here, the estimation was accomplished by studying the time behavior of the derivative D of the mean-value of predators $\langle N \rangle$. From the scaling laws it can be shown that [23],

$$D = \frac{d \log \langle N \rangle}{d \log c} \simeq t^{1/\nu_{\parallel}}, \quad (7)$$

at the critical value of c . Data for different values of c , close to the critical point, were taken in the same run

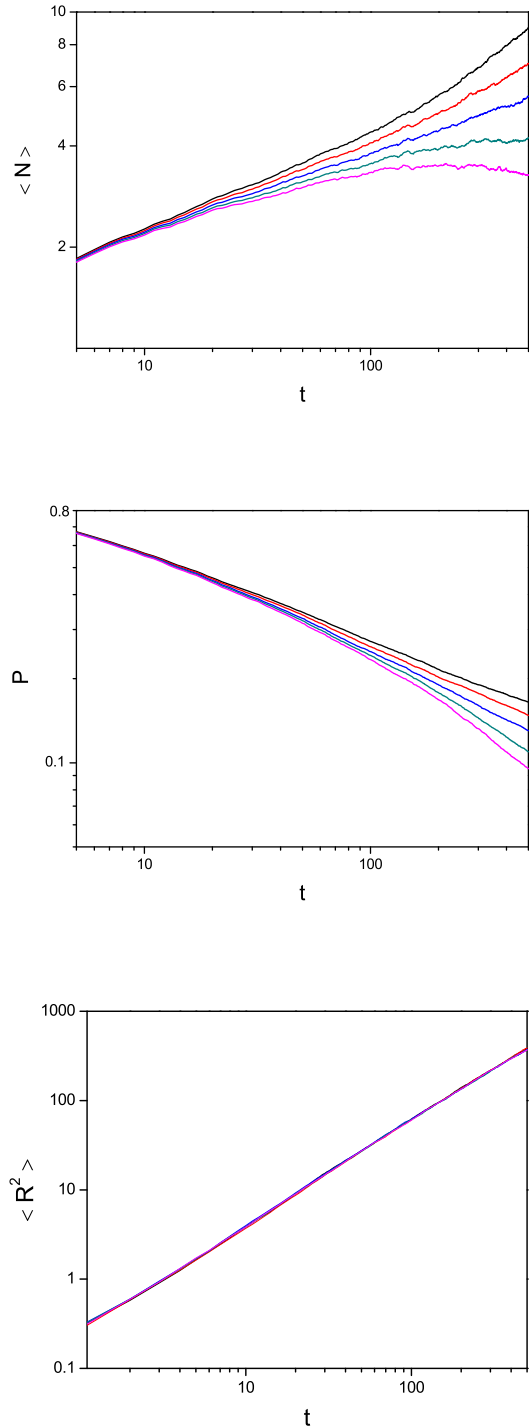


FIG. 2: Log-log plot of the mean-number of predators $\langle N \rangle$ (upper panel), the survival probability P (middle panel) and the mean-square distance of spreading of predators $\langle R^2 \rangle$ (lower panel), as a function of the time t , for $p = 0$. Each figure shows the behavior of these quantities for different values of c . From top to bottom: $c = 0.18875$, $c = 0.18975$, $c = 0.19075$, $c = 0.19175$ and $c = 0.19275$.

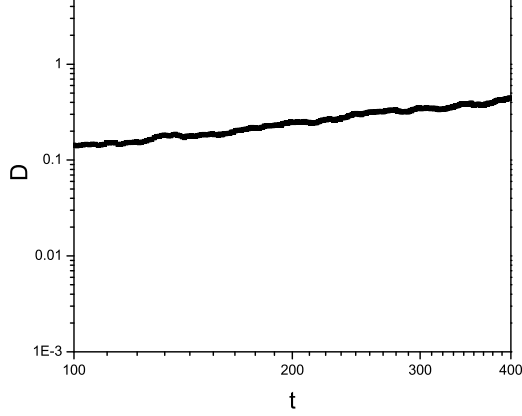


FIG. 3: Logarithmic derivative D of $\langle N \rangle$ with respect to c . For $p = 0$ and considering values of c slightly above and below the critical value.

TABLE I: Phase boundaries and dynamic critical exponents for the predator-prey cellular automaton. The values of the last column were obtained using $\beta = \delta\nu_{\parallel}$.

p	c	η	δ	z	ν_{\parallel}	β
-0.495	0.00206(3)	0.234(4)	0.444(6)	1.13(2)	1.30(2)	0.58(2)
-0.45	0.0228(3)	0.227(4)	0.448(4)	1.13(1)	1.31(2)	0.59(1)
-0.40	0.04515(10)	0.229(3)	0.451(3)	1.135(8)	1.30(1)	0.586(8)
-0.30	0.0877(2)	0.226(3)	0.452(3)	1.134(7)	1.29(1)	0.583(8)
-0.20	0.12695(2)	0.232(2)	0.452(3)	1.129(8)	1.288(9)	0.582(8)
-0.10	0.1617(2)	0.234(3)	0.447(3)	1.135(6)	1.295(10)	0.579(8)
0.00	0.19075(10)	0.230(2)	0.451(3)	1.134(4)	1.292(8)	0.583(7)
0.10	0.2127(2)	0.230(2)	0.449(3)	1.131(7)	1.287(8)	0.578(7)
0.20	0.2243(2)	0.228(2)	0.450(3)	1.128(8)	1.291(9)	0.581(8)
0.22	0.2253(2)	0.231(2)	0.447(3)	1.131(7)	1.29(1)	0.58(1)
0.24	0.2262(2)	0.230(3)	0.445(5)	1.136(9)	1.30(1)	0.58(1)
0.26	0.2263(2)	0.226(4)	0.443(6)	1.129(8)	1.29(1)	0.57(1)
0.28	0.2262(2)	0.232(4)	0.444(6)	1.135(10)	1.29(1)	0.57(1)
0.30	0.2257(1)	0.231(4)	0.445(5)	1.13(1)	1.295(10)	0.58(1)
0.32	0.2250(2)	0.233(4)	0.448(5)	1.14(1)	1.30(1)	0.58(1)
0.34	0.2239(2)	0.234(5)	0.449(6)	1.13(1)	1.29(1)	0.58(1)
0.36	0.223(1)	0.235(7)	0.452(8)	1.14(2)	1.28(2)	0.58(2)
0.38	0.223(2)	0.24(1)	0.44(1)	1.14(2)	1.29(2)	0.57(2)
a	c_c	η	δ	z	ν_{\parallel}	β
0.00	0.220(3)	0.587(2)	0.096(4)	1.767(5)	1.51(1)	0.145(7)
						0.139(4) [†]

[†]See Sec. III D.

and the derivatives calculated considering finite differences; the behavior of D , for $p = 0$, is shown in Fig. 3. As reported in Table I, the value obtained for the exponent ν_{\parallel} , along the transition line, is in agreement with the estimated value $\nu_{\parallel} = 1.295(6)$ [29] for the directed percolation in $2 + 1$ dimensions.

The static exponent β associated to the order parameter



FIG. 4: Two snapshots of the predator-prey automaton, generated from a single predator at the origin (center) of a lattice covered by prey, for $p = -0.45$ and $c = 0.01$ (upper panel, taken at $t = 10000$) and $c = 0.0227$ (lower panel, taken at $t = 65000$). The white points represent sites occupied by prey, the red points by predators and the blue points are empty sites.

ter was calculated from the values for the dynamic critical exponents δ and ν_{\parallel} and using the scaling relation $\beta = \delta\nu_{\parallel}$ [19, 27]. The resulting value for the exponent β , reported on Table I, is consistent with directed percolation in $2 + 1$ dimensions [29].

For sets of parameters such that a approaches zero the critical behavior of the model suggests a crossover to another universality class. This feature will be explored in Sec. III.

C. Growing clusters of predator-prey coexistence

The pictures shown in Figs. 4, 5, and 6 are related to configurations generated by simulations of the predator-prey cellular automaton departing from the initial condition with one predator at the origin and the lattice full of prey. It can be seen in Fig. 4 a configuration in the supercritical regime (upper panel) and an almost critical configuration (lower panel) for a set of parameters which corresponds to $b \ll a$ and $c \ll a$ (left down corner of the triangular phase diagram of Fig. 1). In this case,

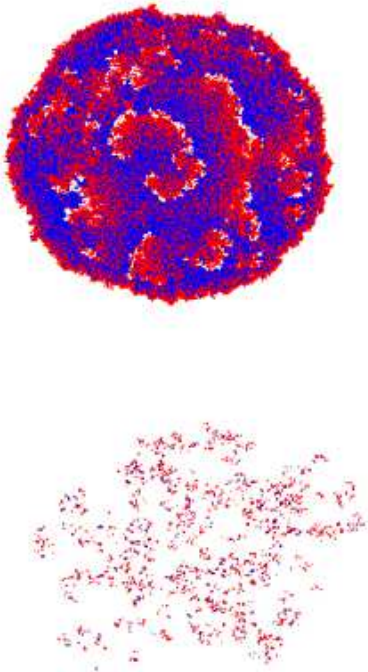


FIG. 5: The same of Fig. 4, for $p = -0.3$ and $c = 0.0075$ (upper panel, taken at $t = 1750$), and $c = 0.0867$ (lower panel, taken after $t = 20000$).

predators stay in the lattice for a long period of time, and when one of them dies it gives place to an empty site that will be almost immediately occupied by a prey individual. Consequently, just a few number of empty sites are present in the steady state and also in the growing clusters. This behavior suggests that the present three state process, in the limit $b \rightarrow 0$, $c \rightarrow 0$ with b/c finite, can be replaced by a two state process, similar to the contact process, involving predators and prey, as pointed out in reference [14].

The growing cluster of the upper panel of Fig. 5 shows a pattern formation related to an active region where prey and predators coexist and can exhibit local time coupled oscillations. With a nonzero probability, the dynamics will survive forever with the densities of each species different from zero but less than 1. This cluster, as well as the supercritical growing clusters of Figs. 4 and 6 (upper panels), assumes after some time, which we call τ , the asymptotic shape of a ball. The correlation length ξ can be understood as the linear size of the cluster at $t = \tau$ so that for $t > \tau$ the system is close to the stationary active state. Our results suggest that the radius R of the ball grows linearly with t for $t > \tau$ in accordance with the shape theorem [16]. At the critical point, τ and ξ diverges. Far from the critical point, the time τ the cluster takes to get a defined shape can be very small.

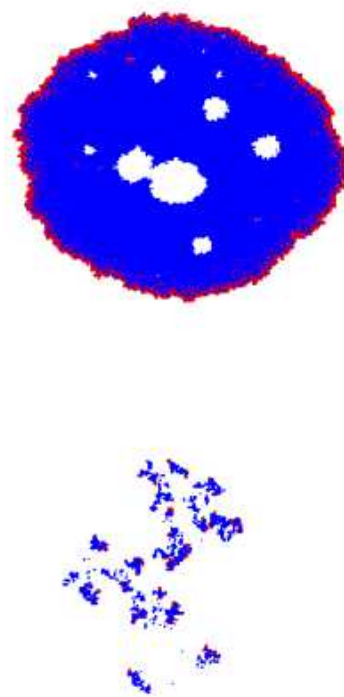


FIG. 6: The same of Fig. 4, for $p = 0.3$ and $c = 0.06$ (upper panel, taken at $t = 500$), and $c = 0.2257$ (lower panel, taken at $t = 3000$).

For instance, for the set of parameters considered in the upper panel of Fig. 6 the shape of a ball is already taken after just 200 time steps.

We notice that the supercritical cluster of Fig. 6 corresponds to a configuration where the populations of prey and predators, under conditions of low densities, are grouped into small clusters of a unique species that are isolated from each other, and coexist without extinction in a highly heterogeneous space. In this respect, this species coexistence can be compared to the Huffaker's experiment, commented in Sec. I. The coexistence for the set of parameters of Fig. 6 is associated to local self-sustained coupled time oscillations of prey and predators populations and has been described in detail in reference [14].

Typical clusters at criticality are shown in the lower panels of Figs. 4, 5 and 6. According to our results of Sec. II A, these configurations must be related with transitions belonging to the universality class of directed percolation. They do not present a ball shape, as the supercritical clusters described above, but rather a shape of a fractal nature. We note that the critical cluster of Fig. 6 (lower panel) presents, in contrast with those of Figs. 4 and 5 (lower panels), noticeable agglomerations of empty sites. For values of p corresponding to small values of a , and, therefore, inside the crossover region, the

III. SPREADING OF AN EPIDEMIC

A. The model

For $a = 0$ the predator-prey probabilistic cellular automaton can be interpreted as a model for the propagation of an epidemic with immunization. It mimics the spreading of an epidemic in a population composed by susceptible individuals (X) that become infected (Y) by contact with infected individuals; once infected the individuals can recover, and become immune (Z) spontaneously. The process of infection can be represented by the reaction:



and the recovery process, which includes immunization, by the reaction:



These are the basic processes which are taken into account in the modeling of the spreading of an epidemics with immunization [20, 21, 32, 33, 34]. The present model is defined on a regular square lattice where each site can be in the following states: occupied by a susceptible, an infected or an immune individual. It comprehends the following stochastic rules:

(A) The infection can occurs when a susceptible individual, which occupy a given site, has at least one site occupied by an infected individual in its neighborhood, reaction (8). This process occurs with probability $b/4$ times the number of infected individuals in the neighboring sites.

(B) The recovering process can occurs spontaneously with probability c when a site is occupied by an infected individual, reaction (9). The condition $b + c = 1$ is obeyed, with b being the infection probability and c the recovery probability. This model can exhibits infinitely many absorbing states and presents a continuous transition belonging to the dynamic percolation universality class, as we show in Sec. III C.

B. Patterns of spreading

To characterize the threshold of the epidemic spreading we perform time-dependent simulations. Initially all sites of the lattice are occupied by susceptible individuals except one, in the origin (center) of the lattice, which is occupied by an infected individual. The stochastic dynamics follows the rules (A) and (B) defined in Sec. III A with a synchronous updating. The infection starts to be transmitted at time $t = 0$. The problem is to know how an epidemic propagates (or not) in the population. For high values of the probability b of infection compared to the values of the recovering probability c , the epidemic spreads leaving a cluster of inactive sites composed by immune individuals and some groups of individuals which

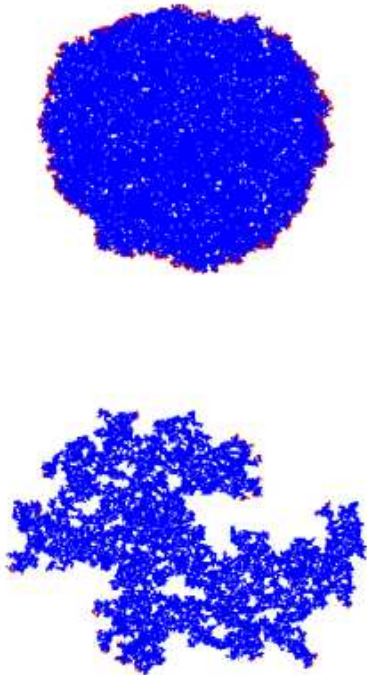


FIG. 7: Two snapshots of the epidemic with immunization ($a = 0$) generated from a single infected individual located at the origin (center) of a lattice covered by susceptible individuals, for $c = 0.15$ (upper panel, taken at $t = 500$) and for $c = 0.22$ (lower panel, taken at $t = 1000$). The white, red and blue points represent sites occupied by susceptible, infected and an immune individuals, respectively.

critical clusters present larger agglomerations of empty sites. In the first time steps of the simulation, they resemble the critical growing cluster for $a = 0$ (lower panel of Fig. 7). However, as long as the parameter a is different from zero, even if it is very small, the critical cluster will present agglomerations of empty sites which can be always active, inasmuch as prey can always proliferate in empty sites. We remark that these critical clusters are still related to transitions belonging to the directed percolation class.

A qualitative similar behavior of critical clusters was obtained by Dammer and Hinrichsen [34] for an epidemic spreading model which also presents a crossover from the directed percolation critical behavior to the dynamic percolation critical behavior.

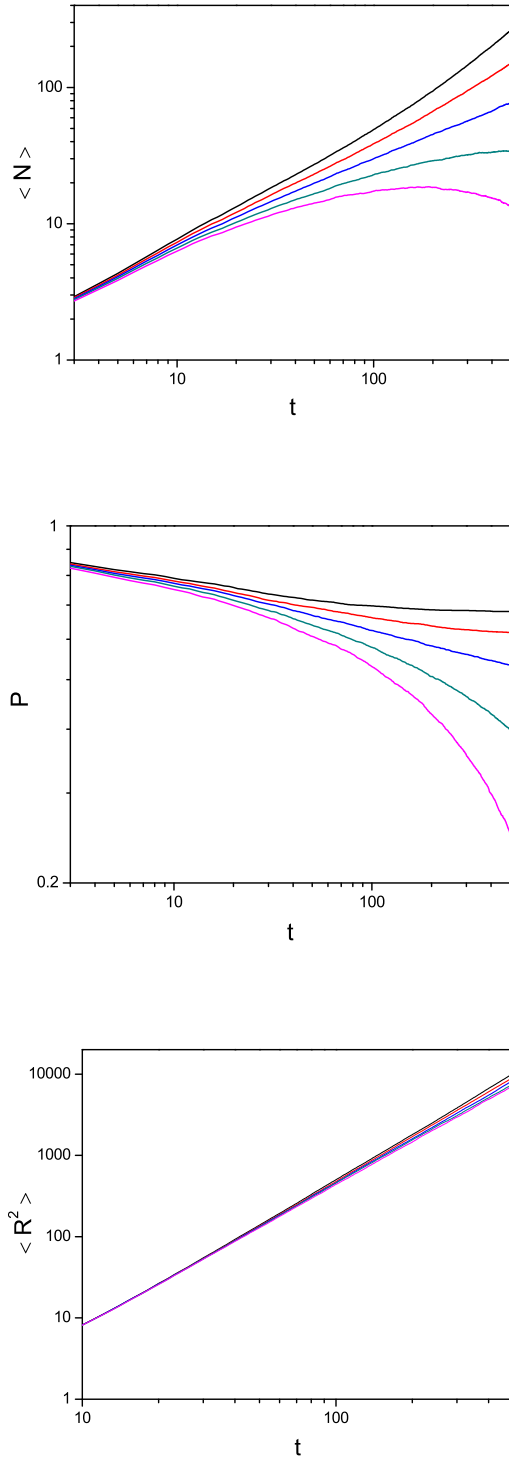


FIG. 8: Log-log plot of the mean-number of infected (upper panel), the survival probability (middle panel) and the mean-square distance of spreading of infected (lower panel), for $a = 0$. Each figure shows the behavior of the quantities for different values of c . From top to bottom: $c = 0.210, 0.215, 0.220, 0.225$ and 0.230 .

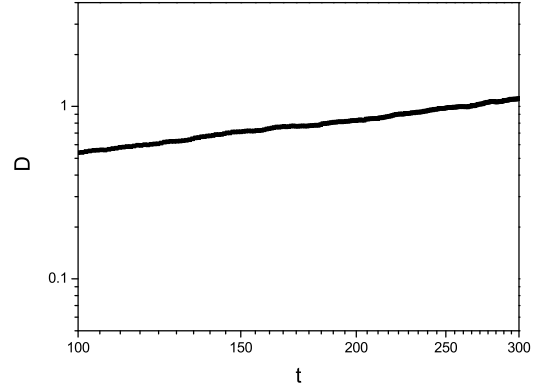


FIG. 9: Logarithmic derivative D of $\langle N \rangle$ with respect to c . For $a = 0$ and considering values of c close to the critical value.

remain susceptible forever. A typical picture of the lattice in this situation is shown in the upper panel of Fig. 7. The cluster grows with a front of infected individuals which stay in the border. After a finite time τ , the cluster assumes a limiting shape of a ball which spreads to infinity with a nonzero probability. We observe that different initial seeds lead to different configurations of the spreading of the epidemic, giving rise to an infinitely many absorbing states. As b is decreased (and c is increased) the threshold for the spreading of the epidemics is reached. Above the threshold, the epidemic will cease in a finite time leaving a cluster with just a few number of immune individuals, the rest of the lattice being covered by susceptible individuals. A picture of the lattice near the threshold of epidemic spreading is shown in the lower panel of Fig. 7. This almost critical cluster presents an irregular shape of fractal nature.

Similar critical and supercritical clusters have been obtained from time-dependent simulations for other spatial-structured stochastic models for an epidemic with immunization [16, 27, 34].

C. Dynamic critical exponents

In Fig. 8 it is shown the time behavior of the mean-number of infected individuals $\langle N \rangle$, the survival probability P , and the mean-square distance of spreading from the origin $\langle R^2 \rangle$ obtained from time-dependent simulations performed near the critical point. Since the log-log plots of these quantities show very clear power-law behavior, associated to critical behavior, then the dynamic critical exponents η , δ and z , defined in Eqs. (4), (5) and (6), can be obtained with precision. The estimated critical exponents are reported in Table I. These exponents are consistent with the critical exponents of the dynamic percolation universality class [29]. This is the expected

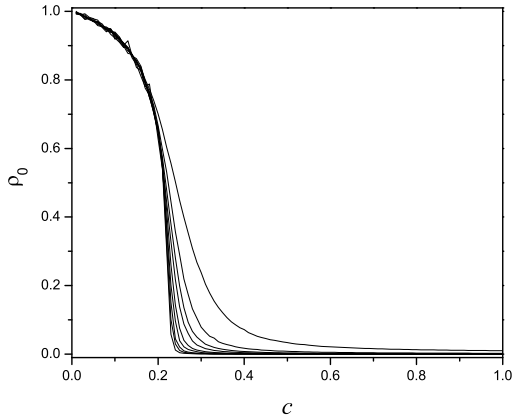


FIG. 10: Density of immune individuals ρ_0 as a function of c , for $a = 0.0$. From top to bottom (at right): $L = 10, 20, 30, 40, 60, 80, 120, 160, 240$. The critical value of c for the infinite system is $c_c = 0.220(3)$ (see Table I).

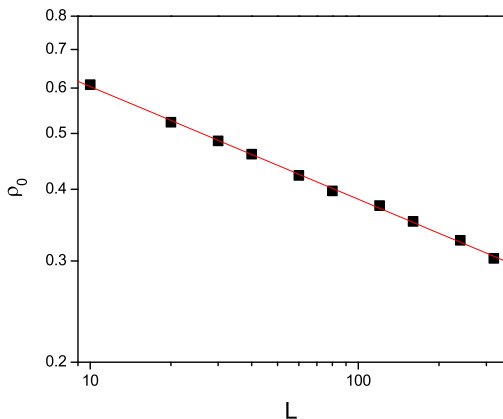


FIG. 11: Log-log plot of ρ_0 , calculated at the critical value $c_c = 0.220$, for $a = 0.0$, as a function of L . Simulations were performed on square lattices of size ranging from $L = 10$ until 320, and considering periodic boundary conditions.

critical universal behavior for a general epidemic with immunization [20, 21].

The critical exponent ν_{\parallel} was obtained by analyzing the behavior of the derivative D , defined in Eq. (7), at the critical point. From Fig. 9 we obtain the estimation $\nu_{\parallel} = 1.51(1)$ which is consistent with the value $\nu_{\parallel} = 1.506(1)$ [29] of the dynamic percolation in two dimensions. The static critical exponent β associated to the order parameter can be evaluated from the estimates for the dynamic critical exponents using the scaling relation $\beta = \delta\nu_{\parallel}$. The resulting value, which is given in Table I, is in agreement with the one for the dynamic

percolation [29]. We also have estimated this exponent by performing steady state simulations in finite systems, as described in the next section.

D. Critical exponent β

To obtain another estimation of the critical exponent β associated to the order parameter we have considered square lattices with linear size L and periodic boundary conditions. For each value of L we have performed several independent simulations runs all starting from a lattice covered with susceptible individuals with the exception of one infected at the center of the lattice. The system evolves in time according to the synchronous stochastic dynamics defined in Sec. III A. In principle, any one of the infinitely many absorbing states can be reached; and, consequently, the number of immune individuals at the steady state varies from sample to sample. A simulation is finished when the system enters in an absorbing state and then the number of immune individuals is calculated. The mean value of this quantity, divided by the total number of lattice sites L^2 , is the density ρ_0 of immune individuals at the steady state (for a given lattice size).

The behavior of ρ_0 as a function of c , for different values of L is shown in Fig. 10. In the subcritical regime (c above its critical value c_c) ρ_0 decreases as L is increased and in the limit $L \rightarrow \infty$ it vanishes. In the supercritical regime ρ_0 is almost independent of L . We have assumed that ρ_0 is an appropriate order parameter for this transition. Assuming the finite size scaling hypothesis [28] we expect that $\rho_0(\Delta, L)$, where $\Delta = c - c_c$, calculated for each value of L , scales at the critical point as,

$$\rho_0(0, L) \sim L^{-\beta/\nu_{\perp}}, \quad (10)$$

where ν_{\perp} is the critical exponent related to the spatial correlation length.

To obtain the ratio β/ν_{\perp} we plot $\log \rho_0$, calculated at c_c , versus $\log L$, as shown in Fig. 11. We obtain $\beta/\nu_{\perp} = 0.185(5)$. Using the result $\nu_{\perp} = 4/3$ [29] we find the value $\beta = 0.139(4)$ which is in agreement with the one for the isotropic percolation, namely $\beta = 5/36$ [29]. And, also in agreement with the value estimated in Sec. III C.

IV. SUMMARY

We have studied a spatial-structured model in which prey and predators individuals reside on the sites of a lattice and are described by discrete dynamic variables. The system evolves in time according to a probabilistic cellular automaton which takes into account the Lotka-Volterra interactions by the use of Markovian local rules. The model exhibits an active phase where prey and predator coexist without extinction, an absorbing prey phase, and, when the birth probability of prey vanishes, a

phase with infinitely many absorbing states composed by empty (immune) sites and prey (susceptible). In the last case, it is more appropriate to refer to the predator-prey cellular automaton as a model for the spreading of an epidemic with immunization in a population composed by susceptible, infected and immune individuals. The automaton was studied by time-dependent simulations which allow us to determine with precision the phase boundaries (thresholds) and the dynamic critical exponents. We have localized a transition line which crosses the entire phase diagram. For all sets of parameters such that the prey birth probability is different from zero, this line separates the active phase, where prey and predators coexist, and the prey absorbing phase. We have shown that this transition belongs to the directed percolation universality class. We also have shown that when the prey birth probability equals zero, there is a crossover to

the universality class of the dynamic percolation.

Patterns of growing clusters with coexistence of prey, predators and empty sites (or, susceptible, infected and immune individuals), generated by the time dependent simulations, in the critical and in the supercritical regimes, were shown and discussed. The present study provides a detailed description of the thresholds of stable coexistence of the two species (or, the spreading of an epidemics) in the context of this predator-prey cellular automaton.

Acknowledgements

The authors have been supported by the Brazilian agency CNPq.

-
- [1] C. B. Huffaker, *Hilgardia* **27**, 343 (1958).
 - [2] R. Durrett and S. Levin, *Theor. Popul. Biol.* **46**, 363 (1994); *J. Theor. Biol.* **205**, 201 (2000).
 - [3] K. Tainaka, *Phys. Rev. Lett.* **63**, 2688 (1989).
 - [4] J. Satulovsky and T. Tomé, *Phys. Rev. E* **49**, 5073 (1994).
 - [5] N. Boccara, O. Roblin, and M. Roger, *Phys. Rev. E* **50**, 4531 (1994).
 - [6] A. Provata, G. Nicolis and F. Baras, *J. Chem. Phys.* **110**, 8361 (1999).
 - [7] T. Antal and M. Droz, *Phys. Rev. E* **63**, 056119 (2001).
 - [8] T. Antal, M. Droz, A. Lipowsky, and G. Odor, *Phys. Rev. E* **64**, 036118 (2001).
 - [9] O. Ovaskainen, K. Sato, J. Bascompe, and I. Hanski, *J. Theor. Biol.* **215**, 95 (2002).
 - [10] M. A. M. Aguiar, E. M. Rauch, and Y. Bar-Yam, *Phys. Rev. E* **67**, 047102 (2003).
 - [11] K. C. de Carvalho and T. Tomé, *Mod. Phys. Lett. B* **18**, 873 (2004).
 - [12] G. Szabó and G. A. Sznaider, *Phys. Rev. E* **69**, 031911 (2004).
 - [13] M. Mobilia, I. T. Georgiev and U. C. Täuber, *Phys. Rev. E* **73**, 040903 (2006).
 - [14] K. C. de Carvalho and T. Tomé, *Self-organized patterns of coexistence out of a predator-prey cellular automaton*. Submitted to publication, q-bio PE/0604030 (2006).
 - [15] T. M. Liggett, *Interacting Particle Systems* (Springer, New York, 1985).
 - [16] R. Durrett, *Lecture Notes on Particle Systems and Percolation* (Wadsworth and Brooks, Pacific Grove, 1988).
 - [17] A. Lotka, *J. Am. Chem. Soc.* **42**, 1595 (1920); *Proc. Nat. Acad. Sci. USA* **6**, 410 (1920); *Elements of Mathematical Biology* (Dover, New York, 1924).
 - [18] V. Volterra, *Leçons sur la Théorie Mathématique de la Lutte pour la Vie*, (Gauthier-Villars, Paris, 1931).
 - [19] P. Grassberger and A. de la Torre, *Ann. Phys.* **122**, 373 (1979).
 - [20] P. Grassberger, *Math. Biosci.* **63**, 157 (1983).
 - [21] J. L. Cardy and P. Grassberger, *J. Phys. A* **18**, L267 (1985).
 - [22] P. Grassberger, *J. Phys. A* **22**, 3673 (1989).
 - [23] P. Grassberger and Y.-C. Zhang, *Physica A* **224**, 189 (1996).
 - [24] I. Jensen, H. C. Fogedby, and R. Dickman, *Phys. Rev. A* **41**, 3411(1990).
 - [25] R. Dickman and T. Tomé, *Phys. Rev. A* **44**, 4833 (1991).
 - [26] I. Jensen, *Phys. Rev. A* **45**, 563 (1992); *Phys. Rev. A* **46**, 7393 (1992).
 - [27] H. Hinrichsen, *Adv. Phys.* **49**, 815 (2000); *Braz. J. Phys.* **30**, 69 (2000).
 - [28] J. Marro and R. Dickman, *Nonequilibrium Phase Transitions* (Cambridge University Press, Cambridge, 1999).
 - [29] M. A. Muñoz, R. Dickman, A. Vespignani and S. Zapperi, *Phys. Rev. E* **59**, 6175 (1999).
 - [30] E. Arashiro and J. R. Drugowich de Felício, *Braz. J. Phys.* **30**, 677(2000).
 - [31] R. da Silva, R. Dickman and J. R. Drugowich de Felício, *Phys. Rev. E* **70**, 067701 (2004).
 - [32] N. Boccara and K.Y. Cheong, *J. Phys. A* **27**, 1585 (1993).
 - [33] A. Hastings, *Population Biology: Concepts and Models*, (Springer, New York, 1997).
 - [34] S. M. Dammer and H. Hinrichsen, *Phys. Rev. E* **68**, 016114 (2003); *J. Stat. Mech.: Theor. Exp.* P07011, 2004.
 - [35] E. Domany and W. Kinzel, *Phys. Rev. Lett.* **53**, 447 (1984).
 - [36] P. Grassberger, *J. Stat. Phys.* **79**, 13 (1995).
 - [37] T. Tomé, E. Arashiro, J. R. Drugowich de Felício, and M. J. de Oliveira, *Braz. J. Phys.* **33**, 458 (2003).
 - [38] R. Ziff, E. Gulari, and Y. Barshad, *Phys. Rev. Lett.* **56**, 2553 (1986).